hearts

MDPI

Review

Optical Mapping in hiPSC-CM and Zebrafish to Resolve Cardiac Arrhythmias

Bert Vandendriessche [1], Ewa Sieliwonczyk [1], Maaike Alaerts [1], Bart L. Loeys [1], Dirk Snyders [2] and Dorien Schepers [1,2,*]

[1] Center of Medical Genetics, Faculty of Medicine and Health Sciences, University of Antwerp and Antwerp University Hospital, Prins Boudewijnlaan 43/6, 2650 Edegem, Belgium; bert.vandendriessche@uantwerpen.be (B.V.); ewa.sieliwonczyk@uantwerpen.be (E.S.); maaike.alaerts@uantwerpen.be (M.A.); bart.loeys@uantwerpen.be (B.L.L.)

[2] Laboratory of Molecular, Cellular and Network Excitability, Department of Biomedical Sciences, University of Antwerp, Universiteitsplein 1, 2610 Wilrijk, Belgium; dirk.snyders@uantwerpen.be

* Correspondence: dorien.schepers@uantwerpen.be

Received: 2 December 2020; Accepted: 16 December 2020; Published: 21 December 2020

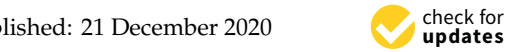

Abstract: Inherited cardiac arrhythmias contribute substantially to sudden cardiac death in the young. The underlying pathophysiology remains incompletely understood because of the lack of representative study models and the labour-intensive nature of electrophysiological patch clamp experiments. Whereas patch clamp is still considered the gold standard for investigating electrical properties in a cell, optical mapping of voltage and calcium transients has paved the way for high-throughput studies. Moreover, the development of human-induced pluripotent stem-cell-derived cardiomyocytes (hiPSC-CMs) has enabled the study of patient specific cell lines capturing the full genomic background. Nevertheless, hiPSC-CMs do not fully address the complex interactions between various cell types in the heart. Studies using in vivo models, are therefore necessary. Given the analogies between the human and zebrafish cardiovascular system, zebrafish has emerged as a cost-efficient model for arrhythmogenic diseases. In this review, we describe how hiPSC-CM and zebrafish are employed as models to study primary electrical disorders. We provide an overview of the contemporary electrophysiological phenotyping tools and discuss in more depth the different strategies available for optical mapping. We consider the current advantages and disadvantages of both hiPSC-CM and zebrafish as a model and optical mapping as phenotyping tool and propose strategies for further improvement. Overall, the combination of experimental readouts at cellular (hiPSC-CM) and whole organ (zebrafish) level can raise our understanding of the complexity of inherited cardiac arrhythmia disorders to the next level.

Keywords: optical mapping; hiPSC-CM; zebrafish; arrhythmia; channelopathies

1. Introduction

Inherited cardiac arrhythmias (ICAs) are a heterogeneous group of rare disorders often characterised by a structural normal heart despite the presence of disease-specific electrocardiographic deviations. The basis for these deviations is frequently found in the genes encoding for the cardiac ion channels and their subunits, which contain rare pathogenic variants. As a result, the normal physiological functioning of these channels is altered, which disturbs the ionic homeostasis inside the cardiomyocytes (CMs) and affects the cardiac action potential (AP). Hence, an arrhythmogenic substrate arises which increases the risk of life-threatening arrhythmias and consequent sudden cardiac death, even in prior asymptomatic young patients [1,2]. Long QT syndrome (LQTS), short QT syndrome (SQTS), Brugada syndrome (BrS) and catecholaminergic polymorphic

ventricular tachycardia (CPVT) are the four major channelopathies. The reported prevalence of channelopathies is often an underestimation because of the presence of asymptomatic mutation carriers, low penetrance, variable expressivity within and between families and diagnostic difficulties as changes in electrocardiogram (ECG) patterns are transient [1–3]. Due to this, elucidating the pathophysiological mechanisms behind the ICAs and identifying patients remains challenging. Over the past two decades, molecular genetic screening of affected individuals and their families has become a standard genetic practice and significantly aids in overcoming the aforementioned hurdles [4]. However, in BrS for instance, only in around 20–25% of the cases can a genetic diagnosis be obtained, leaving a large grey area of BrS patients without a clear pathogenetic mechanism [5]. Therefore, there is an urgent need for improved functional models and techniques to further aid in understanding the aetiology of ICA [6–11].

2. Human-Induced Pluripotent Stem-Cell-Derived Cardiomyocytes (hiPSC-CMs) as a Model for ICA

Since the discovery by Yamanaka and colleagues on how to generate hiPSCs out of somatic cells, the technique has been implemented in a wide variety of fields, including the cardiovascular [12]. Somatic cells can be reprogrammed to a pluripotent state by adding pluripotency-associated genes such as NANOG, OCT4, SOX2 and LIN28 or C-MYC. Numerous somatic cells from patients and healthy individuals have been successfully reprogrammed and differentiated to generate hiPSC-CMs [13,14].

2.1. Differentiation of hiPSC into CM

The first reported differentiation from hiPSCs into hiPSC-CMs was based on embryoid body formation. Unfortunately, differentiation efficiencies were low [15]. Soon after, timed delivery of small molecules was introduced to initiate mesoderm lineage development and consequent CM differentiation, which greatly enhanced efficiencies [16–18]. Crucial to this process is a timed stimulation and inhibition of the Wnt-pathway to initiate and direct differentiation of the hiPSCs towards hiPSC-CMs. Protocols use different molecules, variable concentrations and timings. In general, to start the differentiation process, the Wnt pathway is indirectly activated through inhibition of glycogen synthase kinase 3β (e.g., addition of CHIR99021 molecule to the culture medium). Subsequently, after culturing for a couple of days, a Wnt pathway inhibitor is added to the culture medium (e.g., Wnt-C59 or IWR1). By day seven or eight, the cultured cells start beating spontaneously, which is one of the first signs of differentiation towards CMs [19]. Functional characterisation of the hiPSC-CMs is performed after at least thirty days of culturing to improve maturation [20].

2.2. Functional Assessment of hiPSC-CM: From Patch Clamp to Multi-Electrode Arrays

Since it has been introduced by Neher and Sakmann, the path clamp technique has been the gold standard to functionally assess the electrophysiological activity and the corresponding main ion currents: sodium (Na^{2+}), calcium (Ca^{2+}) and potassium (K^{+}) [21–24]. The main parameters that are analysed in an action potential (AP) are resting membrane potential (RMP), AP amplitude (APA), maximum upstroke velocity (dV/dt_{max}) and AP duration at various repolarisation levels (APD20, −50 and −90) (Figure 1). Despite the abundant information on the AP retrieved via patch clamp, the technique remains laborious and time-consuming. In addition, it requires intensive training and a dedicated set-up. Hence, efforts have been made to automate the technique and measure in parallel [25]. The advent of the planar patch clamp method facilitated the automation process for a large part, resulting in the development of the automated patch clamp (APC) [25,26]. Cells are seeded on top of a glass substrate chip containing one or multiple micro apertures. Applying negative pressure from beneath the apertures will suck the cell towards the opening and block them. Consequently, similar to the manual single-cell patch clamp, the cell membrane is ruptured to gain whole cell access. In the intracellular solution beneath the rupture, a recording electrode is connected to an amplifier to measure the currents. Coupling the planar patch clamp method to automated microfluidic system and even up

to two times 384 multiwell plates facilitates vast parallel recordings, culminating in up to 20,000 data points a day [25,27,28]. In the field of drug discovery and safety testing, APC has gained more attention due to its high-throughput characteristics [29,30]. Nevertheless, combining APC with hiPSC-CM is still proven to be difficult especially because of the intercell variability found between batches of hiPSC-CM. Moreover, the electrophysiological immaturity of hiPSC-CM creates additional challenges in read-out standardisation. Lastly, giga-ohm seals are more difficult to obtain, which significantly reduces the quality of the measurements due to leaky currents [31]. To overcome these limitations, APC has been used in combination with heterologous overexpression systems (e.g., CHO and HEK293 cells) to assess the effect of multiple genetic variants found in LQTS and BrS patients, but obviously these systems are less translational to the human in vivo situation [25,32,33]. Lastly, the high costs associated with the APC systems remain a main hurdle for academia [34].

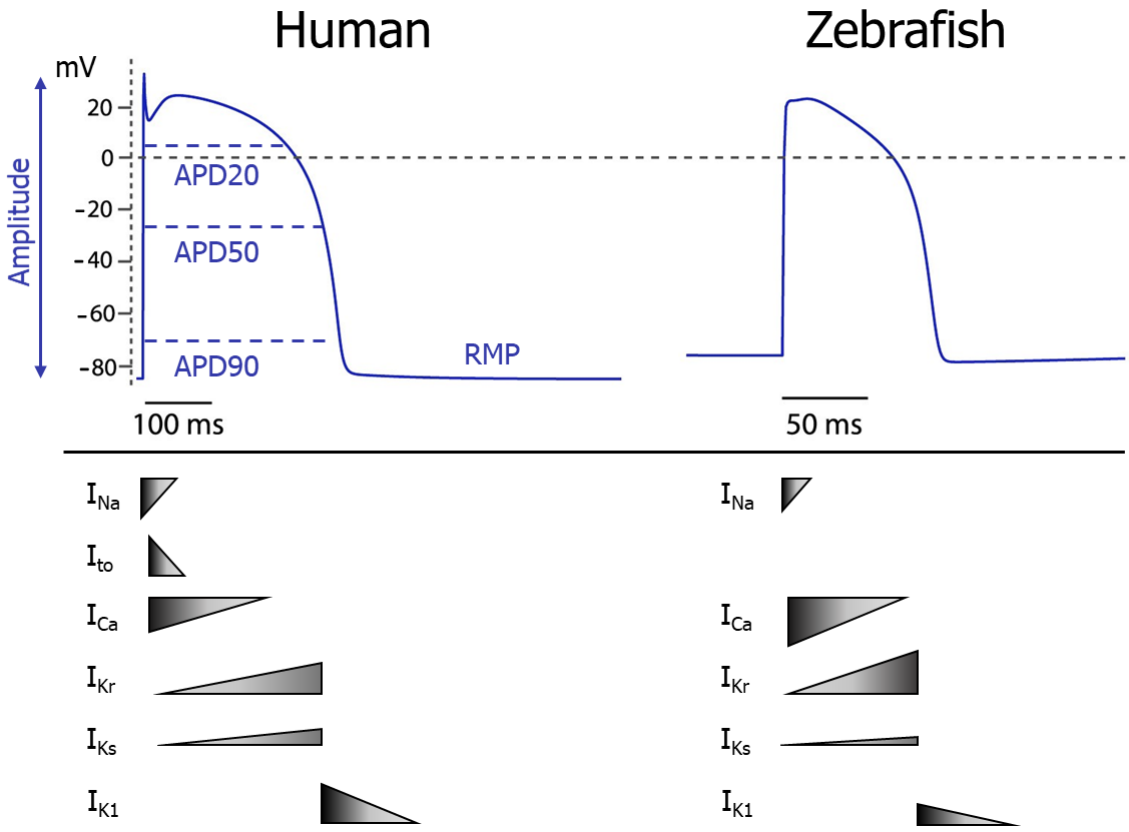

Figure 1. Comparison between human and zebrafish ventricular action potential. At the top, the ventricular action potential shape is depicted in both human and zebrafish. The bottom shows the relative magnitude of the main ion currents that contribute to the different phases of the action potential. APD20, −50 and −90 = action potential duration at 20, 50 or 90% repolarisation, RMP = resting membrane potential, I_{Na} = sodium current, I_{to} = transient outward potassium current, I_{Ca} = calcium current, I_{Kr} = rapidly delayed rectifier potassium current, I_{Ks} = slow delayed rectifier potassium current, I_{K1} = inward rectifier potassium current. Figure adapted from Van Opbergen et al. [35].

In parallel with APC, micro-electrode arrays (MEAs) provide a faster electrophysiological characterisation compared with conventional patch clamp. MEA systems use culture plates containing dot-like electrodes arranged in 2D grids. These electrodes measure beating frequency, conductivity and spatiotemporal, electrical fluctuations in the cell layer recorded as an extracellular field potential (FP). FPs arise from the AP conduction through the cell layer and are therefore similar to an ECG of the human heart, but at a much smaller scale [36]. FPs correlate well with the AP duration and are also used in drug-toxicity screenings [37]. Moreover, the MEA system is suited to perform longitudinal, non-invasive studies on hiPSC-CM. Lastly, the MEA electrodes can be used to pace the hiPSC-CM,

which facilitates synchronous beating at a set frequency throughout the well, and, if used over a prolonged period of time, improves maturation of the hiPSC-CM [38,39]. Nevertheless, FPs remain an indirect way to assess electrical activity inside the hiPSC-CMs. Hence, detailed specific effects on individual ion currents cannot be characterised.

3. Zebrafish as a Model for ICA

Originating from the fresh waters of Southeast Asia, the zebrafish (*Danio rerio*) are an established animal research model in various fields, including cardiovascular research [40,41]. They share >70% of genetic homology with humans and even up to 84% of disease-related genes [42,43]. The major assets for zebrafish use in research are high fecundity, fast and extrauterine development, larval optical transparency and a completely characterised genome with an existing versatile genomic toolbox [41].

3.1. The Zebrafish Heart Electrophysiology

Situated ventral to the oesophagus, the two-chambered zebrafish heart receives deoxygenated venous blood from the sinus venosus. Upon contraction, the blood will be pumped from the atrium to the ventricle and consequently via the bulbus arteriosus to the gills and the rest of the body in a single blood circulation circuit [44]. The heart is one of the first organs that forms straight after insemination. At 24 hours post-fertilisation (hpf), a primitive heart tube already beats, driven by a pacemaker area closely resembling the sino-atrial node (SA node) found in the human heart. At 48 hpf, the cardiac looping is initiated with a clear delineation between the atrial and ventricular components of the heart tube [45]. As in humans, a conduction delay is seen in the atrioventricular (AV) region to allow filling of the ventricle, although no dedicated AV node is present [46]. The His–Purkinje system is not found in zebrafish although ventricular trabeculae will function as a fast conduction system and drive the apex-to-base depolarisation of the heart [35,45]. Beating rate in zebrafish larvae is reported to range from 130 to 180 beats-per-min (bpm) and in adults between 110 and 130 bpm, which is much closer to humans (60–70 bpm) than the 500–600 bpm reported in mice [35,47–51]. On an electrophysiological level, the zebrafish ventricular AP contains the typical plateau phase that is also found in humans but absent in mice. For the main ion currents that drive the AP in humans, zebrafish orthologues are present. The initiation of the AP consists of the rapid upstroke, upon CM stimulation, which is driven by I_{Na}. In zebrafish, this current is created by two sodium channel orthologues but with a lower density than in humans, resulting in a slightly slower upstroke velocity. The following fast repolarisation, driven by I_{to} in humans, is not found in zebrafish. The consequent I_{Ca}, responsible for maintaining the plateau phase, is more dominant than in humans. The L-type calcium channels (LTCCs) are coded by a single human orthologue. Unlike in humans, also the T-type calcium channels contribute toward the ventricular AP in zebrafish, but to a lesser extent [35,52]. For the repolarising potassium channels, creating the I_{Kr} and I_{Ks}, zebrafish orthologues have been identified. For the I_{Kr}, the zebrafish ether-a-go-go-related (zERG) channels have highly similar kinetics as the human ERG (hERG1) channels, coded by *KCNH2*, which mainly drive the repolarisation phase of the ventricular AP [35]. Targeting the zERG2 gene (human *KCNH2* orthologue) in zebrafish resulted in QT prolongation or shortening as seen in LQTS or SQTS [35,53–55]. Transcripts coding for the I_{Ks}-linked potassium channels (K_V 7.1) have also been found in zebrafish although they have not yet been functionally observed [56]. Lastly, in zebrafish a robust I_{K1} is present to sustain the RMP via the Kir2 channels. However, subunit composition differs significantly from the human formation [57,58]. Overall, compared with other (small-sized) animal models, the electrophysiology of the zebrafish heart is one of the closest to humans, as seen in the ECG and AP characteristics. For a more detailed electrophysiological view, comparing the zebrafish to the human heart, excellent reviews exist [35,58,59].

3.2. Functional Assessment of Zebrafish Hearts: Patch Clamp and ECG

Different techniques have been developed to functionally assess the zebrafish heart [60]. Similar to hiPSC-CMs, characterisation of the zebrafish CMs was first performed with the conventional

patch-clamp technique. Recordings were conducted ex vivo on whole zebrafish hearts or on isolated atrial and ventricular CMs [61–64]. In addition, ECG recordings of whole zebrafish hearts have been performed both ex vivo and in vivo with different techniques (e.g., AgCl wire electrodes, suction electrodes and sharp microelectrodes) (Figure 2C) [60,65–68]. Strikingly, the zebrafish ECG strongly resembles the human ECG. The P-wave (depolarisation atrium), the QRS complex (depolarisation ventricle) and the T-wave (repolarisation ventricle) are all visible. Recording electrodes can be positioned on the zebrafish skin or with penetration of the dermal layer and even the pericardial sac. The more invasive techniques increase the sensitivity [66]. The quality of the ECG signal is highly dependent on the positioning of the electrodes and therefore requires trained personnel [48,68]. Additionally, it does not provide a direct measurement of AP. Taking advantage of the optical transparency of zebrafish larvae, it was obvious to take the search for less invasive electrophysiological characterisation methods to the field of optical mapping.

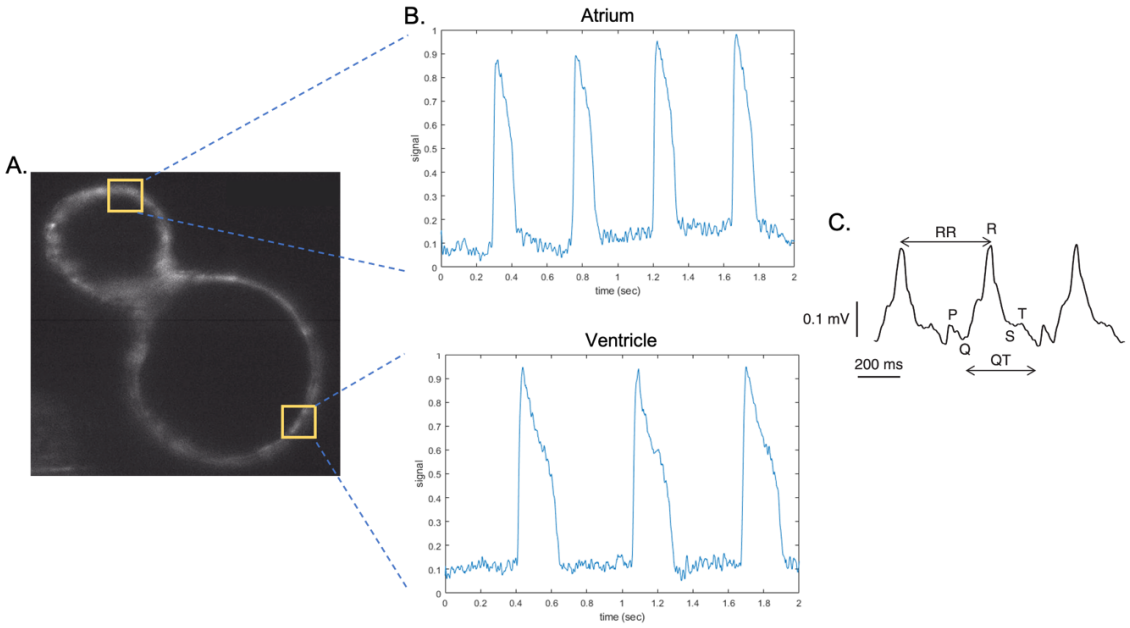

Figure 2. Optical mapping and ECG of the zebrafish heart. (**A**). Section of the heart of a 3 dpf zebrafish embryo expressing the Ace2n-mNeonGreen voltage sensor. The yellow squares indicate the areas in which fluorescence intensity is analysed to obtain the sample traces in (**B**). (**B**). Action potentials from a 3 dpf zebrafish embryo obtained with light sheet microscope. Top: atrial sample trace. Bottom: ventricular sample trace. (**C**). A raw ECG recording of a 2 dpf zebrafish embryo; P, Q, R, S, T waves, and RR and QT intervals indicated. (Figure modified from Thorsen et al. [69]).

4. Optical Mapping

Optical mapping encompasses a broad spectrum of techniques that mostly refer to visualising electrophysiological activity in the CMs or the whole heart by means of fluorescent dyes or genetically encoded fluorescent indicators (GEFIs) (Figure 2A,B). Single wavelength non-ratiometric indicators will report relative changes of a parameter, while dual wavelength ratiometric indicators will visualise absolute changes. The ability to measure a specific electrophysiological parameter will always rely on the interplay between the amount of indicator present and the technical limitations of the detection device to maintain a sufficient signal-to-noise ratio (SNR) [60,70]. For optical mapping studies involving ICAs, two main physiological processes are monitored in CMs: changes in membrane potential and Ca^{2+} transients.

4.1. Imaging Techniques for Electrophysiological Phenotyping

Three main detection set-ups are commonly used to visualise electrophysiological activity in vitro and in vivo: epifluorescence (wide-field) microscopes (EFMs), confocal laser scanning microscopes (CLSMs) and light-sheet fluorescence microscopes (LSFMs) (Table 1). The most widely used is the EFM since it requires the least dedicated set-up. In general, a specific light source is needed which can be either the more traditional mercury, xenon or halogen lamps, although durability, ease-of-use and instability are drawbacks of these bulbs. Nowadays, light-emitting diodes (LEDs) are the illumination source of choice, as they are stable, easy to use and energy efficient with a wide wavelength spectrum that facilitates multi-parametric measurements. Depending on the light source, the in-series positioning of additional shutters, dichroic mirrors, specific wavelength filters and objective lenses will create a light with a unique excitation wavelength, which illuminates the whole sample (EFM and CLSM) or specific areas (LSFM). Charge-coupled device (CCD) cameras or photon-multiplier tubes (PMTs) and derivatives are the most commonly used detection systems [71,72]. Cardiomyocytes will often be seeded as a single cell suspension or in a monolayer. Therefore, the traditional EFM is very well suited for functionally assessing CMs in vitro to capture fluctuations in Ca^{2+} and membrane potential, respectively generating Ca^{2+} transients and APs. Characterisation of CMs as 3D aggregate or the whole heart ex or in vivo poses a challenge for the traditional EFM mainly, as out of focus emitted light will reduce the SNR. To circumvent this, CLSM uses lasers as a light source and a detection system with pinhole micro apertures and PMTs. As in EFM, the whole sample is illuminated. However, due to the pinholes, only the emitted light coming from a confocal point in the sample will reach the detector. Hence, out-of-focus light will not be detected, which greatly increases the SNR. Traditionally, information is gathered by illuminating one position after the other (pixel to pixel) until a 3D image of the sample is reconstructed. However, this is usually too slow to capture rapidly fluctuating events such as Ca^{2+} transients and especially APs. Therefore, the line scan method is used; i.e., the laser scans the same line, but only in a specific plane, for a certain amount of time at frequencies up to 1kHz [70,72]. For in vivo imaging, the main problem with the CLSM is the high intensity of the laser. Phototoxicity and bleaching are known issues due to whole-sample illumination, which can effect temporal resolution. The latter can be circumvented by using LSFM. Different variants of LSFM exist but they all share common features. The illumination and detection path can be modified independently and are orthogonally positioned, which reduces detection of out-of-focus light. In between, a specialised sample holder is present that receives a thin sheet of light (100–200 nm) created by either cylindrical lenses (static light sheet) or galvanometric mirrors (dynamic light sheet). The laser emulates a light sheet by scanning the focal plane with a Gaussian beam of light. By moving the sample through the light sheet, different planes of the samples will be illuminated. Hence, optical sectioning of the sample can be achieved similar to in CLSM [73,74]. The limiting factor for data acquisition in LSFM is the scanning speed of the laser (dynamic light sheet) and the acquisition speed of the camera. Commercial LSFMs can, at best, reach up to 500–600 frames-per-second (fps) which is sufficient for measuring Ca^{2+} transients but is sub-optimal for detecting changes in the fast upstroke velocities of the APs [74]. Subtle changes in AP upstroke velocity are found in BrS patients due to the reduced Na^{2+} current. Nevertheless, some modified LSFMs nowadays reach up to 1000 fps which would be sufficient to detect these changes [75].

Table 1. Advantages and disadvantages of optical mapping techniques in human-induced pluripotent stem-cell-derived cardiomyocyte (hiPSC-CM) and zebrafish. Epifluorescence microscopy (EFM), confocal laser scanning microscopy (CLSM), light-sheet fluorescence microscopy (LSFM).

Method	Advantages	Disadvantages	References
Video recording	Easy to perform	Limited info (heart rate)	hiPSC-CM [76] Zebrafish [77]
EFM	Easy to perform Ideal for 2D cell monolayers Add-on on conventional microscopes Available in every lab/university	Background fluorescence Out-of-focus light detection Difficult with 3D structures	hiPSC-CM [78–81] Zebrafish [82]
CLSM	Optical sectioning (3D samples) Little out-of-focus light detection Line scan method Often available in every university	Dedicated set-up High intensity light source Cytotoxic/bleaching (less with line-scan method)	hiPSC-CM [83,84] Zebrafish [62,85]
LSFM	Optical sectioning (3D samples) Minimal out-of-focus light detection Illuminating only the field of focus Live specimen imaging	Very dedicated set-up Not available in every institution Lower throughput	hiPSC-CM (organoid) [86] Zebrafish [73,87,88]

4.2. Fluorescent Dyes

Historically, visualising free Ca^{2+} in the cytosol of CMs or changes in membrane potential was achieved via administration of fluorescent dyes. The Ca^{2+} fluorescent dyes are based on the principles of chelator molecules and consist of two parts: a cavity which traps the free Ca^{2+} and a scaffold retaining the fluorescence properties. Upon binding of free Ca^{2+}, conformational changes are induced which greatly alter the absorbance and fluorescence characteristics of the molecule. To monitor rapid oscillations in intracellular Ca^{2+}, low-affinity and fast kinetics are essential. Two different types of Ca^{2+} dyes exist: ratiometric (e.g., fura-2 and indo-1) and non-ratiometric (e.g., Cal520 and fluo-4) dyes. The former have two distinct wavelength excitation or emission spectra from which a ratio can be constructed that quantitatively correlates with change in Ca^{2+} concentrations. The latter only have a single-wavelength excitation/emission spectrum [70]. Although no quantitative measurements can be made, their fluorescence intensity can change up to a hundred-fold upon Ca^{2+} binding which results in a far greater SNR compared to the ratiometric dyes [89]. Equipping the dyes with a lipophilic acetoxymethyl (AM) ester group facilitates an easy transmembrane uptake into the cell. Once inside, the ester groups are cleaved-off and the dye is trapped inside. The introduction of this technique greatly reduced the concerns about dye-leakage out of the cells and made them more suitable for reliable longitudinal studies [70].

Visualising rapid changes in membrane potential is achieved by voltage fluorescent dyes that can respond in pico-microseconds. Two main classes exist: electrochromic indicators (e.g., di-4ANNEPS and derivatives) and photo-induced electron transfer (PeT)-based dyes (e.g., Fluovolt). They both contain a hydrophobic part to be incorporated into the cell membrane [90]. The first class will, upon detecting depolarisation in the membrane, undergo a charge shift inside the probe which results in a small wavelength shift in absorption and emission. Despite their ultrafast kinetics (femto-to picoseconds), only a small fluorescence intensity change can be measured, resulting in a low SNR. The second class relies on PeT, which is a slower (microseconds) mechanism but with a far greater change in fluorescence intensity. Upon depolarisation, the electron-rich quencher can no longer transfer electrons to the attached, excited-state fluorophore which results in a detectable signal. Repolarisation restores the electric field in the membrane and the electrons can transfer to the active fluorophore to

quench it [91]. However, some cytotoxic effects of long-term imaging with this second class of dyes have been reported [90]. Despite the good signal of PeT-based indicators, Ca^{2+} dyes retain the best SNR as they localise in a larger volume (i.e., cytosol) compared with the membrane-located voltage dyes. Therefore, they are less affected by bleaching and are more suited for longitudinal studies [92].

4.3. Genetically Encoded Voltage/Calcium Indicators

In order to circumvent the drawbacks of fluorescent dyes, e.g., non-homogenous dyes loading, time-consuming staining protocols, cytotoxicity and inability to target specific cell types, genetically encoded fluorescent indicators (GEFI) were developed [70,93]. Comparable to the dyes, both genetically encoded Ca^{2+} (GECI) and voltage (GEVI) indicators exist. The GECIs can be categorised in two big groups based on the number of fluorophores. In general, a Ca^{2+}-binding scaffold (e.g., calmodulin-M13 peptide pair or troponin C domain) is combined with one or two fluorophores, resulting in non-ratiometric and ratiometric indicators, respectively [70]. Additionally, blue, green and red fluorescent indicators create further sub-categories [90]. The most widely used GECIs are the ones from the GCaMP family. These non-ratiometric GECIs can rely on fast association and dissociation kinetics with a high SNR ratio upon binding Ca^{2+} [90]. The second group of Ca^{2+} indicators are the "cameleons" and rely on the principle of fluorescence resonance energy transfer (FRET). Upon binding Ca^{2+}, a conformational change will bring both fluorophores in close proximity of one another. The emitted light from the first excited fluorophore will now be able to excite the second fluorophore. Similar to the dyes, a ratio can be constructed to quantitate the change in Ca^{2+} concentration [70].

For the GEVIs, three main classes exist which can also be subcategorised based on their fluorophore or ratiometric properties. The first ones are based on the voltage sensing domain of voltage sensitive phosphatases. In general, this class is characterised by slower kinetics (millisecond range) but with good SNR (e.g., ArcLight and derivatives) [94]. The second class of GEVIs is derived from microbial opsins, i.e., rhodopsins. These mutated opsins are capable of responding to changes in membrane potential in the sub-millisecond range (e.g., Arch, QuasAr and derivatives). The protonation of the opsin's retinal cofactor will be altered upon sensing voltage changes, generating differences in fluorescence intensity of the protein. Despite their fast kinetics, their fluorescent intensity is relatively dim compared to the other classes [95]. The third class of GEVIs counters the inherent dimness of the rhodopsins by attaching fluorophores to them (e.g., Ace-mNeonGreen and derivatives). Based on the FRET principles, the rhodopsin functions as quencher for the excited fluorophore, depending on the membrane potential. The coupling of the fluorophore slightly reduces the kinetics of the GEVI. Nevertheless, they are still close to sub-millisecond range with an SNR almost as good as the first GEVI class [95]. One exciting characteristic from GEFIs is that they can easily be combined in a single cell. Different subtypes of GECI and GEVIs exist that are active or emit light in the red and near-infrared emission spectrum. The emitted light at this end of the spectrum is of a longer wavelength; hence, absorption and scattering are also reduced [96,97]. With a dedicated fluorescent microscope set-up, simultaneous recording of Ca^{2+} transients and membrane potentials can be achieved [80,85,98].

4.4. Optical Mapping in hiPSC-CM and Zebrafish to Model ICAs

The above techniques have been used frequently in the past decade to characterise ICAs both in hiPSC-CM and zebrafish hearts. They offer a valid alternative or are used complementary to the conventional electrophysiological patch clamping techniques [85,99–103]. So far, characterising ICAs in hiPSC-CM solely via optical mapping is not yet an established practice. Usually, patch clamp in combination with MEA or optical mapping is used. From all the optical techniques, Ca^{2+} imaging via fluorescent dyes in hiPSC-CMs is regularly implemented to characterise all four major channelopathies (Table 2). In the transparent zebrafish larvae, complementary fluorescence imaging of the whole heart as a method to functionally assess ICAs has been used in LQTS [53,82,104,105], SQTS [106] and cardiac conduction-system disease (CCSD) (Table 2) [107]. ECG recordings or (high-speed) light microscopy videos (i.e., monitoring heart rate) of non-transparent adult zebrafish have been utilised for the study

of LQTS [54,108,109], SQTS [69] and BrS [110]. Most recent development and implementation of state-of-the-art fluorescence microscopy techniques and GEFIs enable reliable in vivo optical mapping in the whole heart of zebrafish larvae [85,101,103].

Table 2. Overview of optical mapping methods used to study ICAs in hiPSC-CMs and zebrafish. Inherited cardiac arrhythmias (ICA), long QT syndrome (LQTS), Brugada syndrome (BrS), catecholaminergic polymorphic ventricular tachycardia (CPVT), short QT syndrome (SQTS), genetically encoded calcium indicator (GECI), genetically encoded voltage indicator (GEVI).

ICA	Model	Calcium		Voltage	
		Dye	GECI	Dye	GEVI
LQTS	hiPSC-CM	Fluo-4 AM [81,111–114] Fura-2 AM [115]	/	/	Arclight [111,116]
	Zebrafish	Calcium Green Dextran [82,104]	gCaMP [53]	di-4 ANEPPS [105]	/
BrS	hiPSC-CM	Fluo-4 AM [117,118] Fluo-3 AM [119]	/	/	/
CPVT	hiPSC-CM	Fluo-4 AM [83,120–124] Fura-2 AM [125]	GCaMP6f-Junctin [126]	/	/
SQTS	hiPSC-CM	Fluo-3 AM [127,128]	FluoVolt [129]	/	/
	Zebrafish	Calcium Green Dextran [106]		/	/

5. Limitations, Challenges and Future of Optical Mapping in hiPSC-CM and Zebrafish

5.1. hiPSC-CMs: From Immaturity to Organoids

Despite their numerous advantages and applications, even in drug-toxicity research, hiPSC-CMs still suffer from their immature phenotype [100,130]. Morphologically, they are smaller and have a round shape in contrast to the rod-shaped adult iPSC-CMs. On a structural level, iPSC-CMs lack a fully organised myofilament system and sarcoplasmic reticulum that lies in close proximity to the cell membrane, which facilitates an efficient excitation–contraction coupling. They are spontaneously beating, a feature found in foetal and nodal iPSC-CMs but not in native atrial and ventricular CMs. Lastly, on an electrophysiological level, the resting membrane potential (RMP) is positively shifted (−60 to −40 mV instead of −80 mV) mainly due to the absence of the inwardly rectifier potassium current (I_{K1}) [131–133]. Therefore, continuous efforts are being made to improve differentiation protocols and increase maturation. For instance, supplementing the culture medium with the thyroid hormone T3, electrical pacing, culturing on micropatterned scaffolds, increasing culture times and timed introduction of metabolic selection media (e.g., lactate) have all been reported to stabilise intracellular organisation and improve maturation in hiPSC-CMs [130–133]. At present, the aforementioned maturity issues, differences between differentiation protocols and batch-to-batch variability hamper the widespread use of hiPSC-CMs. Better standardisation of protocols and characterisation strategies will be necessary to further establish the use of hiPSC-CMs in industry and academia [134]. Lastly, in order to fully model the human heart in vitro, efforts are being made to create cardiac organoids in 3D, i.e., engineered heart tissue in a dish. As in the whole heart, multiple cell types contribute to and sustain the proper functioning of the organ. Co-culturing the CMs with cardiac endothelial cells and fibroblast should allow paracrine regulation and the interaction with extracellular matrix, respectively [135]. Furthermore, differentiating the individual cell types from a patient's hiPSC line would create an even more translational in vitro model. Optical mapping is ideally suited to characterise these dense 3D models, which would be more challenging with the conventional patch clamp techniques [100].

5.2. Modelling ICAs in Zebrafish Models

The biggest difference between the human and the zebrafish heart is that structurally the latter one only contains two chambers instead of four. In order to model BrS, this might pose a challenge as the right ventricular outflow tract (RVOT) is indicated as the onset region to induce arrhythmia in humans. One potential explanation is the observation that the I_{to} current is more prominently present in the epicardium of this region than in the endocardium. This creates a transmural voltage gradient larger than in any other region of the ventricles [1]. In the zebrafish heart, a RVOT is not present and an I_{to} not found, which would therefore impede modelling of BrS in zebrafish. However, the exact pathological mechanism in BrS is still unclear and only in around 25% of BrS cases a genetic diagnosis can be made [5]. This leaves a large grey area that still can benefit from modelling the disease in an animal with a high electrophysiological resemblance to the human heart. Early on in evolution, the zebrafish genome underwent a whole-genome duplication (WGD) which resulted in numerous para- and orthologous genes. With an exception of *CACNA1C*, multiple orthologue genes exist that encode the main ion channels regulating the AP in the zebrafish heart [58]. Although this poses an additional challenge to model ICAs, the high homology with the human channels and presence of a dominant isoform of the channel creates opportunities. For instance, LQTS has been successfully re-created in zebrafish by transient knock-down of the zERG2 channel. Co-injection of mRNA coding for the human hERG1 channel was able to partially rescue the phenotype but mRNA containing a LQTS specific mutation was not [54,136]. Lastly, zebrafish cardiomyocytes lack a transverse tubular (T-tubular) system and the Ca^{2+} transient is less dependent on the Ca^{2+} release of the sarcoplasmic reticulum as seen in humans. The RyR2 channels are also markedly less sensitive to free Ca^{2+}. Therefore, Ca^{2+} handling needs to be further investigated to be able to fully model CPVT for example. GECIs would be ideally suited to further study this in more detail as they can visualise Ca^{2+} release on a subcellular level [35].

5.3. Technical Challenges and Future Directions of Optical Mapping

The most challenging part about optical mapping is mitigating motion artefacts coming from the contracting cardiomyocytes, which would constantly alter the background fluorescence levels. One way to achieve this is by using ratiometric indicators, as they will both suffer from motion artefacts. The ratio between the indicators should therefore cancel out the artefact although this is technically challenging [137]. Another way is by decoupling the electrical from the mechanical activity. Hence, the propagating AP and consequent Ca^{2+} release can still be monitored without inducing myofilament activity. Blebbistatin, a class II myosin inhibitor, was first used to achieve this de-coupling in zebrafish larvae [62]. However, inherent cyto- and phototoxicity, poor water solubility and high fluorescence properties of this inhibitor are serious disadvantages when performing fluorescence imaging. Recently, para-aminoblebbistatin was introduced, which resolved or improved the previous issues [138]. Specific for zebrafish, electromechanical decoupling can also be achieved by knocking down the cardiac troponin T (*TTNT2*) gene using morpholinos [139]. The question remains to which extent this gene knock-down alters other relevant cardiac physiological processes. Lastly, algorithms have been designed that can perform motion tracking and stabilisation and do not require the attachment of additional visible markers to aid the tracking. It only requires the visible textures of the heart to estimate the optical flow between two images. Wide-spread application of this method needs further investigation, but the obvious advantages would lead to modelling in more physiologically relevant conditions via optical mapping [140].

Imaging adult zebrafish is an additional challenge compared to larvae due to the acquired pigmentation. To circumvent this, special zebrafish lines exist with mutations to inhibit pigmentation (e.g., *casper* or *crystal* fish) [141].

Finally, inherent limitations of optical mapping still pose challenges to measure specific AP characteristics. Determining maximum upstroke velocity is hampered as too few data points can be measured, with a good SNR, due to current limitations in data acquisition speed. Technical improvement of voltage dyes, GEVIs and imaging equipment will resolve this. Absolute measurements of membrane

potential (in millivolt) cannot be obtained via fluorescence imaging. One recent report correlates alteration in fluorescence lifetime of the excited fluorophores with resting membrane potential. However, only certain voltage or Ca^{2+} dyes are suited and, therefore, more research is needed on this technique [142]. At present, visualising individual ion currents is also not possible. Nevertheless, current optical mapping techniques already enable the visualisation of a vast amount of (sub)cellular processes, not solely in the heart [95]. Lastly, 3D samples such as organoids and whole zebrafish hearts are coming into the picture as more relevant models to study ICAs. These dense samples pose only minor problems for current fluorescence imaging techniques in comparison to the (micro)electrode-based techniques, which perform measurements on the surface.

6. Conclusions

The advent of hiPSC-CMs and zebrafish as state-of-the-art models to study ICA has facilitated a more personalised and in-depth characterisation of patient-specific mutations. Conventional electrode-based techniques are very well suited for single cell characterisation but are limited in data output when assessing 3D-like structures. Optical mapping, therefore, is a valuable complementary technique to the traditional electrophysiological methods. The recent advances made in the field of fluorescence microscopy and (genetically encoded) indicators not only reduce cytotoxic effects but also greatly improve the signal-to-noise ratio and will facilitate simultaneous recording of both action potentials and calcium transients in vitro and in vivo. Therefore, a bright future lies ahead for optical mapping to aid in the functional characterisation of these study models.

Author Contributions: Writing—original draft preparation, B.V. and E.S.; writing—review and editing, M.A., B.L.L., D.S. (Dirk Snyders), D.S. (Dorien Schepers); funding acquisition, B.L.L., D.S. (Dirk Snyders), D.S. (Dorien Schepers). All authors have read and agreed to the published version of the manuscript.

Funding: This review effort is supported by funding from the Research Foundation Flanders (FWO, Belgium, G0C6220N) and the University of Antwerp (Methusalem-OEC grant "Genomed" FFB190208). B.V. and E.S. are junior investigators supported by the Research Foundation Flanders (FWO, grant numbers 1177421N and 1192019N). B.L.L. is a senior clinical investigator of FWO and holds a consolidator grant from the European Research Council (Genomia—ERC-COG-2017-771945). D.S. (Dorien Schepers) is supported by a postdoctoral fellowship of the Research Foundation Flanders (FWO; grant number 12R5610N).

Conflicts of Interest: The authors declare no conflict of interest.

References

1. Schwartz, P.J.; Ackerman, M.J.; Antzelevitch, C.; Bezzina, C.R.; Borggrefe, M.; Cuneo, B.F.; Wilde, A.A.M. Inherited cardiac arrhythmias. *Nat. Rev. Dis. Prim.* **2020**, *6*, 1–22. [CrossRef]
2. Offerhaus, J.A.; Bezzina, C.R.; Wilde, A.A.M. Epidemiology of inherited arrhythmias. *Nat. Rev. Cardiol.* **2020**, *17*, 205–215. [CrossRef] [PubMed]
3. Wong, C.X.; Brown, A.; Lau, D.H.; Chugh, S.S.; Albert, C.M.; Kalman, J.M.; Sanders, P. Epidemiology of Sudden Cardiac Death: Global and Regional Perspectives. *Hear. Lung Circ.* **2019**, *28*, 6–14. [CrossRef] [PubMed]
4. Wilde, A.A.M.; Nannenberg, E.; Van Der Werf, C. Cardiogenetics, 25 years a growing subspecialism. *Neth. Hear. J.* **2020**, *28*, 39–43. [CrossRef] [PubMed]
5. Monasky, M.M.; Micaglio, E.; Ciconte, G.; Pappone, C. Brugada Syndrome: Oligogenic or Mendelian Disease? *Int. J. Mol. Sci.* **2020**, *21*, 1687. [CrossRef] [PubMed]
6. Betzenhauser, M.J.; Pitt, G.S.; Antzelevitch, C. Calcium Channel Mutations in Cardiac Arrhythmia Syndromes. *Curr. Mol. Pharmacol.* **2015**, *8*, 133–142. [CrossRef] [PubMed]
7. Monasky, M.M.; Pappone, C.; Piccoli, M.; Ghiroldi, A.; Micaglio, E.; Anastasia, L. Calcium in Brugada Syndrome: Questions for Future Research. *Front. Physiol.* **2018**, *9*, 1088. [CrossRef] [PubMed]
8. Hosseini, S.M.; Kim, R.; Udupa, S.; Costain, G.; Jobling, R.; Liston, E.; Jamal, S.M.; Szybowska, M.; Morel, C.F.; Bowdin, S.; et al. Reappraisal of Reported Genes for Sudden Arrhythmic Death. *Circ.* **2018**, *138*, 1195–1205. [CrossRef] [PubMed]

9. Sendfeld, F.; Selga, E.; Scornik, F.S.; Pérez, G.J.; Mills, N.L.; Brugada, R. Experimental Models of Brugada syndrome. *Int. J. Mol. Sci.* **2019**, *20*, 2123. [CrossRef]
10. Wallace, E.; Howard, L.; Liu, M.; O'Brien, T.; Ward, D.; Shen, S.; Prendiville, T. Long QT Syndrome: Genetics and Future Perspective. *Pediatr. Cardiol.* **2019**, *40*, 1419–1430. [CrossRef]
11. Pourrier, M.; Fedida, D. The Emergence of Human Induced Pluripotent Stem Cell-Derived Cardiomyocytes (hiPSC-CMs) as a Platform to Model Arrhythmogenic Diseases. *Int. J. Mol. Sci.* **2020**, *21*, 657. [CrossRef] [PubMed]
12. Yoshida, Y.; Yamanaka, S. Induced Pluripotent Stem Cells 10 Years Later. *Circ. Res.* **2017**, *120*, 1958–1968. [CrossRef] [PubMed]
13. Takahashi, K.; Tanabe, K.; Ohnuki, M.; Narita, M.; Ichisaka, T.; Tomoda, K.; Yamanaka, S. Induction of Pluripotent Stem Cells from Adult Human Fibroblasts by Defined Factors. *Cell* **2007**, *131*, 861–872. [CrossRef] [PubMed]
14. Karagiannis, P.; Takahashi, K.; Saito, M.; Yoshida, Y.; Okita, K.; Watanabe, A.; Inoue, H.; Yamashita, J.K.; Todani, M.; Nakagawa, M.; et al. Induced Pluripotent Stem Cells and Their Use in Human Models of Disease and Development. *Physiol. Rev.* **2019**, *99*, 79–114. [CrossRef] [PubMed]
15. Zhang, J.; Wilson, G.F.; Soerens, A.G.; Koonce, C.H.; Yu, J.; Palecek, S.P.; Thomson, J.A.; Kamp, T.J. Functional Cardiomyocytes Derived From Human Induced Pluripotent Stem Cells. *Circ. Res.* **2009**, *104*, e30–e41. [CrossRef] [PubMed]
16. Ren, Y.; Lee, M.Y.; Schliffke, S.; Paavola, J.; Amos, P.J.; Ge, X.; Ye, M.; Zhu, S.; Senyei, G.; Lum, L.; et al. Small molecule Wnt inhibitors enhance the efficiency of BMP-4-directed cardiac differentiation of human pluripotent stem cells. *J. Mol. Cell. Cardiol.* **2011**, *51*, 280–287. [CrossRef]
17. Lian, X.; Hsiao, C.; Wilson, G.; Zhu, K.; Hazeltine, L.B.; Azarin, S.M.; Raval, K.K.; Zhang, J.; Kamp, T.J.; Palecek, S.P. Cozzarelli Prize Winner: Robust cardiomyocyte differentiation from human pluripotent stem cells via temporal modulation of canonical Wnt signaling. *Proc. Natl. Acad. Sci. USA* **2012**, *109*, E1848–E1857. [CrossRef]
18. Lian, X.; Zhang, J.; Azarin, S.M.; Zhu, K.; Hazeltine, L.B.; Bao, X.; Hsiao, C.; Kamp, T.J.; Palecek, S.P. Directed cardiomyocyte differentiation from human pluripotent stem cells by modulating Wnt/β-catenin signaling under fully defined conditions. *Nat. Protoc.* **2013**, *8*, 162–175. [CrossRef]
19. Zhao, M.; Tang, Y.; Zhou, Y.; Zhang, J. Deciphering Role of Wnt Signalling in Cardiac Mesoderm and Cardiomyocyte Differentiation from Human iPSCs: Four-dimensional control of Wnt pathway for hiPSC-CMs differentiation. *Sci. Rep.* **2019**, *9*, 1–15. [CrossRef]
20. Kumar, N.; Dougherty, J.A.; Manring, H.R.; Elmadbouh, I.; Mergaye, M.; Czirok, A.; Isai, D.G.; Belevych, A.E.; Yu, L.; Janssen, P.M.; et al. Assessment of temporal functional changes and miRNA profiling of human iPSC-derived cardiomyocytes. *Sci. Rep.* **2019**, *9*, 1–16. [CrossRef]
21. Sakmann, B.; Neher, E. Patch Clamp Techniques for Studying Ionic Channels in Excitable Membranes. *Annu. Rev. Physiol.* **1984**, *46*, 455–472. [CrossRef] [PubMed]
22. Neher, E.; Sakmann, B. The Patch Clamp Technique. *Sci. Am.* **1992**, *266*, 44–51. [CrossRef]
23. Laurila, E.; Ahola, A.; Hyttinen, J.; Aalto-Setälä, K. Methods for in vitro functional analysis of iPSC derived cardiomyocytes—Special focus on analyzing the mechanical beating behavior. *Biochim. Biophys. Acta (BBA) Bioenerg.* **2016**, *1863*, 1864–1872. [CrossRef] [PubMed]
24. Garg, P.; Garg, V.; Shrestha, R.; Sanguinetti, M.C.; Kamp, T.J.; Wu, J.C. Human Induced Pluripotent Stem Cell–Derived Cardiomyocytes as Models for Cardiac Channelopathies. *Circ. Res.* **2018**, *123*, 224–243. [CrossRef] [PubMed]
25. Obergrussberger, A.; Friis, S.; Brüggemann, A.; Fertig, N. Automated patch clamp in drug discovery: Major breakthroughs and innovation in the last decade. *Expert Opin. Drug Discov.* **2020**, 1–5. [CrossRef]
26. Dunlop, J.; Bowlby, M.R.; Peri, R.; Vasilyev, D.; Arias, R. High-throughput electrophysiology: An emerging paradigm for ion-channel screening and physiology. *Nat. Rev. Drug Discov.* **2008**, *7*, 358–368. [CrossRef]
27. Obergrussberger, A.; Stölzle-Feix, S.; Becker, N.; Brüggemann, A.; Fertig, N.; Möller, C. Novel screening techniques for ion channel targeting drugs. *Channels* **2015**, *9*, 367–375. [CrossRef]
28. Annecchino, L.A.; Schultz, S.R. Progress in automating patch clamp cellular physiology. *Brain Neurosci. Adv.* **2018**, *2*, 2398212818776561. [CrossRef]

29. Mann, S.A.; Heide, J.; Knott, T.; Airini, R.; Epureanu, F.B.; Deftu, A.-F.; Deftu, A.-T.; Radu, B.M.; Amuzescu, B. Recording of multiple ion current components and action potentials in human induced pluripotent stem cell-derived cardiomyocytes via automated patch-clamp. *J. Pharmacol. Toxicol. Methods* **2019**, *100*, 106599. [CrossRef]
30. Brinkwirth, N.; Takasuna, K.; Doi, M.; Becker, N.; Obergrussberger, A.; Friis, S.; Furukawa, H.; Hasegawa, Y.; Oka, T.; Ohtsuki, A.; et al. Reliable identification of cardiac liability in drug discovery using automated patch clamp: Benchmarking best practices and calibration standards for improved proarrhythmic assessment. *J. Pharmacol. Toxicol. Methods* **2020**, *105*, 106884. [CrossRef]
31. Obergrussberger, A.; Haarmann, C.; Stölzle-Feix, S.; Becker, N.; Ohtsuki, A.; Brüggemann, A.; George, M.; Fertig, N. Automated Patch Clamp Recordings of Human Stem Cell-Derived Cardiomyocytes. In *Bioinformatics in MicroRNA Research*; Springer Science and Business Media LLC: Berlin, Germany, 2016; pp. 57–82.
32. Glazer, A.; Wada, Y.; Li, B.; Muhammad, A.; Kalash, O.R.; O'Neill, M.J.; Shields, T.; Hall, L.; Short, L.; Blair, M.A.; et al. High-Throughput Reclassification of SCN5A Variants. *Am. J. Hum. Genet.* **2020**, *107*, 111–123. [CrossRef] [PubMed]
33. Ng, C.-A.; Perry, M.D.; Liang, W.; Smith, N.J.; Foo, B.; Shrier, A.; Lukacs, G.L.; Hill, A.P.; Vandenberg, J.I. High-throughput phenotyping of heteromeric human ether-à-go-go-related gene potassium channel variants can discriminate pathogenic from rare benign variants. *Hear. Rhythm.* **2020**, *17*, 492–500. [CrossRef] [PubMed]
34. Bell, D.C.; Dallas, M.L. Using automated patch clamp electrophysiology platforms in pain-related ion channel research: Insights from industry and academia. *Br. J. Pharmacol.* **2017**, *175*, 2312–2321. [CrossRef] [PubMed]
35. Van Opbergen, C.J.M.; van der Voorn, S.M.; Vos, M.A.; de Boer, T.P.; van Veen, T.A.B. Cardiac Ca(2+) signalling in zebrafish: Translation of findings to man. *Prog. Biophys. Mol. Biol.* **2018**, *138*, 45–58. [CrossRef] [PubMed]
36. Kussauer, S.; Robert, D.; Lemcke, H. hiPSCs Derived Cardiac Cells for Drug and Toxicity Screening and Disease Modeling: What Micro- Electrode-Array Analyses Can Tell Us. *Cells* **2019**, *8*, 1331. [CrossRef]
37. Millard, D.; Dang, Q.; Shi, H.; Zhang, X.; Strock, C.; Kraushaar, U.; Zeng, H.; Levesque, P.; Lu, H.-R.; Guillon, J.-M.; et al. Cross-Site Reliability of Human Induced Pluripotent stem cell-derived Cardiomyocyte Based Safety Assays Using Microelectrode Arrays: Results from a Blinded CiPA Pilot Study. *Toxicol. Sci.* **2018**, *164*, 550–562. [CrossRef]
38. Ruan, J.-L.; Tulloch, N.L.; Razumova, M.V.; Saiget, M.; Muskheli, V.; Pabon, L.; Reinecke, H.; Regnier, M.; Murry, C.E. Mechanical Stress Conditioning and Electrical Stimulation Promote Contractility and Force Maturation of Induced Pluripotent Stem Cell-Derived Human Cardiac Tissue. *Circulation* **2016**, *134*, 1557–1567. [CrossRef]
39. Wei, F.; Pourrier, M.; Strauss, D.G.; Stockbridge, N.; Pang, L. Effects of Electrical Stimulation on hiPSC-CM Responses to Classic Ion Channel Blockers. *Toxicol. Sci.* **2020**, *174*, 254–265. [CrossRef]
40. Lieschke, G.J.; Currie, P.D. Animal models of human disease: Zebrafish swim into view. *Nat. Rev. Genet.* **2007**, *8*, 353–367. [CrossRef]
41. Bradford, Y.M.; Toro, S.; Ramachandran, S.; Ruzicka, L.; Howe, D.G.; Eagle, A.; Kalita, P.; Martin, R.; Moxon, S.A.T.; Schaper, K.; et al. Zebrafish Models of Human Disease: Gaining Insight into Human Disease at ZFIN. *ILAR J.* **2017**, *58*, 4–16. [CrossRef]
42. Howe, K.; Clark, M.D.; Torroja, C.F.; Torrance, J.; Berthelot, C.; Muffato, M.; Collins, J.E.; Humphray, S.; McLaren, K.; Matthews, L.; et al. The zebrafish reference genome sequence and its relationship to the human genome. *Nature* **2013**, *496*, 498–503. [CrossRef] [PubMed]
43. Ryan, R.; Moyse, B.R.; Richardson, R.J. Zebrafish cardiac regeneration—looking beyond cardiomyocytes to a complex microenvironment. *Histochem. Cell Biol.* **2020**, *154*, 533–548. [CrossRef] [PubMed]
44. Menke, A.L.; Spitsbergen, J.M.; Wolterbeek, A.P.M.; Woutersen, R.A. Normal Anatomy and Histology of the Adult Zebrafish. *Toxicol. Pathol.* **2011**, *39*, 759–775. [CrossRef] [PubMed]
45. Wilkinson, R.N.; Jopling, C.; Van Eeden, F.J.M. Zebrafish as a Model of Cardiac Disease. *Prog. Mol. Biol. Transl. Sci.* **2014**, *124*, 65–91. [CrossRef]

46. Sedmera, D.; Reckova, M.; DeAlmeida, A.; Sedmerova, M.; Biermann, M.; Volejnik, J.; Sarre, A.; Raddatz, E.; McCarthy, R.A.; Gourdie, R.G.; et al. Functional and morphological evidence for a ventricular conduction system in zebrafish and Xenopus hearts. *Am. J. Physiol. Circ. Physiol.* **2003**, *284*, H1152–H1160. [CrossRef]
47. Sarmah, S.; Marrs, J.A. Zebrafish as a Vertebrate Model System to Evaluate Effects of Environmental Toxicants on Cardiac Development and Function. *Int. J. Mol. Sci.* **2016**, *17*, 2123. [CrossRef]
48. Santoso, F.; Farhan, S.M.A.; Castillo, A.L.; Malhotra, N.; Saputra, F.; Kurnia, K.A.; Chen, K.H.-C.; Huang, J.-C.; Chen, J.-R.; Hsiao, C.-D. An Overview of Methods for Cardiac Rhythm Detection in Zebrafish. *Biomedicines* **2020**, *8*, 329. [CrossRef]
49. Giardoglou, P.; Beis, D. On Zebrafish Disease Models and Matters of the Heart. *Biomedicines* **2019**, *7*, 15. [CrossRef]
50. Genge, C.E.; Lin, E.; Lee, L.; Sheng, X.; Rayani, K.; Gunawan, M.; Stevens, C.M.; Li, A.Y.; Talab, S.S.; Claydon, T.; et al. The Zebrafish Heart as a Model of Mammalian Cardiac Function. *Rev. Physiol. Biochem. Pharmacol.* **2016**, *171*, 99–136. [CrossRef]
51. Rayani, K.; Lin, E.; Craig, C.; Lamothe, M.; Shafaattalab, S.; Gunawan, M.; Li, A.Y.; Hove-Madsen, L.; Tibbits, G.F. Zebrafish as a model of mammalian cardiac function: Optically mapping the interplay of temperature and rate on voltage and calcium dynamics. *Prog. Biophys. Mol. Biol.* **2018**, *138*, 69–90. [CrossRef]
52. Haverinen, J.; Hassinen, M.; Dash, S.N.; Vornanen, M. Expression of calcium channel transcripts in the zebrafish heart: Dominance of T-type channels. *J. Exp. Biol.* **2018**, *221*, jeb179226. [CrossRef] [PubMed]
53. Arnaout, R.; Ferrer, T.; Huisken, J.; Spitzer, K.; Stainier, D.Y.R.; Tristani-Firouzi, M.; Chi, N.C. Zebrafish model for human long QT syndrome. *Proc. Natl. Acad. Sci. USA* **2007**, *104*, 11316–11321. [CrossRef] [PubMed]
54. Tanaka, Y.; Hayashi, K.; Fujino, N.; Konno, T.; Tada, H.; Nakanishi, C.; Hodatsu, A.; Tsuda, T.; Nagata, Y.; Teramoto, R.; et al. Functional analysis of KCNH2 gene mutations of type 2 long QT syndrome in larval zebrafish using microscopy and electrocardiography. *Hear. Vessel.* **2019**, *34*, 159–166. [CrossRef] [PubMed]
55. Leong, I.U.S.; Skinner, J.R.; Shelling, A.; Love, D.R. Identification and expression analysis of kcnh2 genes in the zebrafish. *Biochem. Biophys. Res. Commun.* **2010**, *396*, 817–824. [CrossRef]
56. Abramochkin, D.V.; Hassinen, M.; Vornanen, M. Transcripts of Kv7.1 and MinK channels and slow delayed rectifier K+ current (IKs) are expressed in zebrafish (Danio rerio) heart. *Pflügers Arch. Eur. J. Physiol.* **2018**, *470*, 1753–1764. [CrossRef]
57. Hassinen, M.; Haverinen, J.; Hardy, M.E.; Shiels, H.A.; Vornanen, M. Inward rectifier potassium current (I K1) and Kir2 composition of the zebrafish (Danio rerio) heart. *Pflügers Arch. Eur. J. Physiol.* **2015**, *467*, 2437–2446. [CrossRef]
58. Ravens, U. Ionic basis of cardiac electrophysiology in zebrafish compared to human hearts. *Prog. Biophys. Mol. Biol.* **2018**, *138*, 38–44. [CrossRef]
59. Vornanen, M.; Hassinen, M. Zebrafish heart as a model for human cardiac electrophysiology. *Channels* **2016**, *10*, 101–110. [CrossRef]
60. Lin, E.; Shafaattalab, S.; Gill, J.; Al-Zeer, B.; Craig, C.; Lamothe, M.; Rayani, K.; Gunawan, M.; Li, A.Y.; Hove-Madsen, L.; et al. Physiological phenotyping of the adult zebrafish heart. *Mar. Genom.* **2020**, *49*, 100701. [CrossRef]
61. Brette, F.; Luxan, G.; Cros, C.; Dixey, H.; Wilson, C.; Shiels, H.A. Characterization of isolated ventricular myocytes from adult zebrafish (Danio rerio). *Biochem. Biophys. Res. Commun.* **2008**, *374*, 143–146. [CrossRef]
62. Jou, C.J.; Spitzer, K.W.; Tristani-Firouzi, M. Blebbistatin Effectively Uncouples the Excitation-Contraction Process in Zebrafish Embryonic Heart. *Cell. Physiol. Biochem.* **2010**, *25*, 419–424. [CrossRef] [PubMed]
63. Nemtsas, P.; Wettwer, E.; Christ, T.; Weidinger, G.; Ravens, U. Adult zebrafish heart as a model for human heart? An electrophysiological study. *J. Mol. Cell. Cardiol.* **2010**, *48*, 161–171. [CrossRef] [PubMed]
64. Verkerk, A.O.; Remme, C.A. Zebrafish: A novel research tool for cardiac (patho)electrophysiology and ion channel disorders. *Front. Physiol.* **2012**, *3*, 255. [CrossRef] [PubMed]
65. Miranda, M.; Egaña, J.T.; Allende, M.L.; Eblen-Zajjur, A. Myocardial Monophasic Action Potential Recorded by Suction Electrode for Ionic Current Studies in Zebrafish. *Zebrafish* **2019**, *16*, 427–433. [CrossRef]
66. Liu, C.C.; Li, L.; Lam, Y.W.; Siu, C.W.; Cheng, S.H. Improvement of surface ECG recording in adult zebrafish reveals that the value of this model exceeds our expectation. *Sci. Rep.* **2016**, *6*, 25073. [CrossRef]

67. Lin, M.-H.; Chou, H.-C.; Chen, Y.-F.; Liu, W.; Lee, C.-C.; Liu, L.Y.-M.; Chuang, Y.-J. Development of a rapid and economic in vivo electrocardiogram platform for cardiovascular drug assay and electrophysiology research in adult zebrafish. *Sci. Rep.* **2018**, *8*, 15986. [CrossRef]
68. Zhao, Y.; Yun, M.; Nguyen, S.A.; Tran, M.; Nguyen, T.P. In Vivo Surface Electrocardiography for Adult Zebrafish. *J. Vis. Exp.* **2019**, e60011. [CrossRef]
69. Thorsen, K.; Dam, V.S.; Kjaer-Sorensen, K.; Pedersen, L.N.; Skeberdis, V.A.; Jurevicius, J.; Treinys, R.; Petersen, I.M.B.S.; Nielsen, M.S.; Oxvig, C.; et al. Loss-of-activity-mutation in the cardiac chloride-bicarbonate exchanger AE3 causes short QT syndrome. *Nat. Commun.* **2017**, *8*, 1696. [CrossRef]
70. Bruton, J.D.; Cheng, A.J.; Westerblad, H. Measuring Ca2+ in Living Cells. *Adv. Exp. Med. Biol.* **2019**, *1131*, 7–26. [CrossRef]
71. Herron, T.J.; Lee, P.; Jalife, P.M.J. Optical Imaging of Voltage and Calcium in Cardiac Cells & Tissues. *Circ. Res.* **2012**, *110*, 609–623. [CrossRef]
72. Sanderson, M.J.; Smith, I.; Parker, I.; Bootman, M.D. Fluorescence microscopy. *Cold Spring Harb. Protoc.* **2014**, *2014*, pdb top071795. [CrossRef]
73. Power, R.M.; Huisken, J. A guide to light-sheet fluorescence microscopy for multiscale imaging. *Nat. Methods* **2017**, *14*, 360–373. [CrossRef]
74. Elisa, Z.; Toon, B.; De Smedt, S.C.; Katrien, R.; Kristiaan, N.; Braeckmans, K. Technical implementations of light sheet microscopy. *Microsc. Res. Tech.* **2018**, *81*, 941–958. [CrossRef] [PubMed]
75. Chen, B.-C.; Legant, W.R.; Wang, K.; Shao, L.; Milkie, D.E.; Davidson, M.W.; Janetopoulos, C.; Wu, X.S.; Hammer, J.A.; Liu, Z.; et al. Lattice light-sheet microscopy: Imaging molecules to embryos at high spatiotemporal resolution. *Science* **2014**, *346*, 1257998. [CrossRef] [PubMed]
76. Toepfer, C.N.; Sharma, A.; Cicconet, M.; Garfinkel, A.C.; Mücke, M.; Neyazi, M.; Willcox, J.A.; Agarwal, R.; Schmid, M.; Rao, J.; et al. SarcTrack. *Circ. Res.* **2019**, *124*, 1172–1183. [CrossRef] [PubMed]
77. Sala, L.; Van Meer, B.J.; Tertoolen, L.G.; Bakkers, J.; Bellin, M.; Davis, R.P.; Denning, C.N.; Dieben, M.A.; Eschenhagen, T.; Giacomelli, E.; et al. MUSCLEMOTION. *Circ. Res.* **2018**, *122*, e5–e16. [CrossRef] [PubMed]
78. Da Rocha, A.M.; Campbell, K.; Mironov, S.; Jiang, J.; Mundada, L.; Guerrero-Serna, G.; Jalife, J.; Herron, T.J. hiPSC-CM Monolayer Maturation State Determines Drug Responsiveness in High Throughput Pro-Arrhythmia Screen. *Sci. Rep.* **2017**, *7*, 1–12. [CrossRef] [PubMed]
79. Da Rocha, A.M.; Creech, J.; Thonn, E.; Mironov, S.; Herron, T.J. Detection of Drug-Induced Torsades de Pointes Arrhythmia Mechanisms Using hiPSC-CM Syncytial Monolayers in a High-Throughput Screening Voltage Sensitive Dye Assay. *Toxicol. Sci.* **2019**, *173*, 402–415. [CrossRef] [PubMed]
80. Nguyen, C.; Upadhyay, H.; Murphy, M.; Borja, G.; Rozsahegyi, E.J.; Barnett, A.; Brookings, T.; McManus, O.B.; Werley, C.A. Simultaneous voltage and calcium imaging and optogenetic stimulation with high sensitivity and a wide field of view. *Biomed. Opt. Express* **2019**, *10*, 789–806. [CrossRef]
81. Shah, D.; Prajapati, C.; Penttinen, K.; Cherian, R.M.; Koivumäki, J.T.; Alexanova, A.; Hyttinen, J.; Aalto-Setälä, K. hiPSC-Derived Cardiomyocyte Model of LQT2 Syndrome Derived from Asymptomatic and Symptomatic Mutation Carriers Reproduces Clinical Differences in Aggregates but Not in Single Cells. *Cells* **2020**, *9*, 1153. [CrossRef] [PubMed]
82. Pott, A.; Bock, S.; Berger, I.M.; Frese, K.; Dahme, T.; Keßler, M.; Rinné, S.; Decher, N.; Just, S.; Rottbauer, W.; et al. Mutation of the Na+/K+-ATPase Atp1a1a.1 causes QT interval prolongation and bradycardia in zebrafish. *J. Mol. Cell. Cardiol.* **2018**, *120*, 42–52. [CrossRef] [PubMed]
83. Sleiman, Y.; Souidi, M.; Kumar, R.; Yang, E.; Jaffré, F.; Zhou, T.; Bernardin, A.; Reiken, S.; Cazorla, O.; Kajava, A.V.; et al. Modeling polymorphic ventricular tachycardia at rest using patient-specific induced pluripotent stem cell-derived cardiomyocytes. *EBioMedicine* **2020**, *60*, 103024. [CrossRef] [PubMed]
84. Crestani, T.; Steichen, C.; Neri, E.; Rodrigues, M.; Fonseca-Alaniz, M.H.; Ormrod, B.; Holt, M.R.; Pandey, P.; Harding, S.; Ehler, E.; et al. Electrical stimulation applied during differentiation drives the hiPSC-CMs towards a mature cardiac conduction-like cells. *Biochem. Biophys. Res. Commun.* **2020**, *533*, 376–382. [CrossRef] [PubMed]
85. Hou, J.H.; Kralj, J.M.; Douglass, A.D.; Engert, F.; Cohen, A.E. Simultaneous mapping of membrane voltage and calcium in zebrafish heart in vivo reveals chamber-specific developmental transitions in ionic currents. *Front. Physiol.* **2014**, *5*, 344. [CrossRef] [PubMed]

86. Turaga, D.; Matthys, O.B.; Hookway, T.A.; Joy, D.A.; Calvert, M.; McDevitt, T.C. Single-Cell Determination of Cardiac Microtissue Structure and Function Using Light Sheet Microscopy. *Tissue Eng. Part C Methods* **2020**, *26*, 207–215. [CrossRef] [PubMed]
87. Maioli, V.; Boniface, A.; Mahou, P.; Ortas, J.F.; Abdeladim, L.; Beaurepaire, E.; Supatto, W. Fast in vivo multiphoton light-sheet microscopy with optimal pulse frequency. *Biomed. Opt. Express* **2020**, *11*, 6012–6026. [CrossRef] [PubMed]
88. Logan, S.L.; Dudley, C.; Baker, R.P.; Taormina, M.J.; Hay, E.A.; Parthasarathy, R. Automated high-throughput light-sheet fluorescence microscopy of larval zebrafish. *PLoS ONE* **2018**, *13*, e0198705. [CrossRef] [PubMed]
89. Lock, J.T.; Parker, I.; Smith, I. A comparison of fluorescent Ca2+ indicators for imaging local Ca2+ signals in cultured cells. *Cell Calcium* **2015**, *58*, 638–648. [CrossRef]
90. Broyles, C.N.; Robinson, P.; Daniels, M.J. Fluorescent, Bioluminescent, and Optogenetic Approaches to Study Excitable Physiology in the Single Cardiomyocyte. *Cells* **2018**, *7*, 51. [CrossRef]
91. Miller, E.W.; Lin, J.Y.; Frady, E.P.; Steinbach, P.A.; Kristan, W.B.; Tsien, R.Y. Optically monitoring voltage in neurons by photo-induced electron transfer through molecular wires. *Proc. Natl. Acad. Sci. USA* **2012**, *109*, 2114–2119. [CrossRef]
92. Kulkarni, R.U.; Miller, E.W. Voltage Imaging: Pitfalls and Potential. *Biochemistry* **2017**, *56*, 5171–5177. [CrossRef] [PubMed]
93. O'Shea, C.; Kabir, S.N.; Holmes, A.P.; Lei, M.; Fabritz, L.; Rajpoot, K.; Pavlovic, D. Cardiac optical mapping —State-of-the-art and future challenges. *Int. J. Biochem. Cell Biol.* **2020**, *126*, 105804. [CrossRef] [PubMed]
94. Bando, Y.; Grimm, C.; Cornejo, V.H.; Yuste, R. Genetic voltage indicators. *BMC Biol.* **2019**, *17*, 1–12. [CrossRef] [PubMed]
95. Panzera, L.C.; Hoppa, M.B. Genetically Encoded Voltage Indicators Are Illuminating Subcellular Physiology of the Axon. *Front. Cell. Neurosci.* **2019**, *13*, 52. [CrossRef] [PubMed]
96. Shemetov, A.A.; Monakhov, M.V.; Zhang, Q.; Canton-Josh, J.E.; Kumar, M.; Chen, M.; Matlashov, M.E.; Li, X.; Yang, W.; Nie, L.; et al. A near-infrared genetically encoded calcium indicator for in vivo imaging. *Nat. Biotechnol.* **2020**, *2020*, 1–10. [CrossRef]
97. Monakhov, M.V.; Matlashov, M.E.; Colavita, M.; Song, C.; Shcherbakova, D.M.; Antic, S.D.; Verkhusha, V.V.; Knöpfel, T. Screening and Cellular Characterization of Genetically Encoded Voltage Indicators Based on Near-Infrared Fluorescent Proteins. *ACS Chem. Neurosci.* **2020**, *11*, 3523–3531. [CrossRef]
98. Shinnawi, R.; Huber, I.; Maizels, L.; Shaheen, N.; Gepstein, A.; Arbel, G.; Tijsen, A.J.; Gepstein, L. Monitoring Human-Induced Pluripotent Stem Cell-Derived Cardiomyocytes with Genetically Encoded Calcium and Voltage Fluorescent Reporters. *Stem Cell Rep.* **2015**, *5*, 582–596. [CrossRef]
99. Herron, T.J. Calcium and voltage mapping in hiPSC-CM monolayers. *Cell Calcium* **2016**, *59*, 84–90. [CrossRef]
100. Goldfracht, I.; Efraim, Y.; Shinnawi, R.; Kovalev, E.; Huber, I.; Gepstein, A.; Arbel, G.; Shaheen, N.; Tiburcy, M.; Zimmermann, W.-H.; et al. Engineered heart tissue models from hiPSC-derived cardiomyocytes and cardiac ECM for disease modeling and drug testing applications. *Acta Biomater.* **2019**, *92*, 145–159. [CrossRef]
101. Van Opbergen, C.J.; Koopman, C.D.; Kok, B.J.; Knöpfel, T.; Renninger, S.L.; Orger, M.B.; Vos, M.A.; Van Veen, T.A.; Bakkers, J.; De Boer, T.P. Optogenetic sensors in the zebrafish heart: A novel in vivo electrophysiological tool to study cardiac arrhythmogenesis. *Theranostics* **2018**, *8*, 4750–4764. [CrossRef]
102. Lin, E.; Craig, C.; Lamothe, M.; Sarunic, M.V.; Beg, M.F.; Tibbits, G.F. Construction and use of a zebrafish heart voltage and calcium optical mapping system, with integrated electrocardiogram and programmable electrical stimulation. *Am. J. Physiol. Integr. Comp. Physiol.* **2015**, *308*, R755–R768. [CrossRef] [PubMed]
103. Salgado-Almario, J.; Vicente, M.; Vincent, P.; Domingo, B.; Llopis, J. Mapping Calcium Dynamics in the Heart of Zebrafish Embryos with Ratiometric Genetically Encoded Calcium Indicators. *Int. J. Mol. Sci.* **2020**, *21*, 6610. [CrossRef] [PubMed]
104. Meder, B.; Scholz, E.P.; Hassel, D.; Wolff, C.; Just, S.; Berger, I.M.; Patzel, E.; Karle, C.; Katus, H.A.; Rottbauer, W. Reconstitution of defective protein trafficking rescues Long-QT syndrome in zebrafish. *Biochem. Biophys. Res. Commun.* **2011**, *408*, 218–224. [CrossRef] [PubMed]
105. Peal, D.S.; Mills, R.W.; Lynch, S.N.; Mosley, J.M.; Lim, E.; Ellinor, P.T.; January, C.T.; Peterson, R.T.; Milan, D.J.; Elllinor, P.T. Novel Chemical Suppressors of Long QT Syndrome Identified by an In Vivo Functional Screen. *Circulation* **2010**, *123*, 23–30. [CrossRef] [PubMed]

106. Hassel, D.; Scholz, E.P.; Trano, N.; Friedrich, O.; Just, S.; Meder, B.; Weiss, D.L.; Zitron, E.; Marquart, S.; Vogel, B.; et al. Deficient ZebrafishEther-à-Go-Go–Related Gene Channel Gating Causes Short-QT Syndrome in ZebrafishReggaeMutants. *Circulation* **2008**, *117*, 866–875. [CrossRef] [PubMed]
107. Hayashi, K.; Teramoto, R.; Nomura, A.; Asano, Y.; Beerens, M.; Kurata, Y.; Kobayashi, I.; Fujino, N.; Furusho, H.; Sakata, K.; et al. Impact of functional studies on exome sequence variant interpretation in early-onset cardiac conduction system diseases. *Cardiovasc. Res.* **2020**, *116*, 2116–2130. [CrossRef]
108. Da'As, S.I.; Thanassoulas, A.; Calver, B.L.; Beck, K.; Salem, R.; Saleh, A.; Kontogianni, I.; Al-Maraghi, A.; Nasrallah, G.K.; Safieh-Garabedian, B.; et al. Arrhythmogenic calmodulin E105A mutation alters cardiac RyR2 regulation leading to cardiac dysfunction in zebrafish. *Ann. N. Y. Acad. Sci.* **2019**, *1448*, 19–29. [CrossRef]
109. Berchtold, M.W.; Zacharias, T.; Kulej, K.; Wang, K.; Torggler, R.; Jespersen, T.; Chen, J.-N.; Larsen, M.R.; La Cour, J.M. The Arrhythmogenic Calmodulin Mutation D129G Dysregulates Cell Growth, Calmodulin-dependent Kinase II Activity, and Cardiac Function in Zebrafish. *J. Biol. Chem.* **2016**, *291*, 26636–26646. [CrossRef]
110. Juang, J.-M.J.; Binda, A.; Lee, S.-J.; Hwang, J.-J.; Chen, W.-J.; Liu, Y.-B.; Lin, L.-Y.; Yu, C.-C.; Ho, L.-T.; Huang, H.-C.; et al. GSTM3 variant is a novel genetic modifier in Brugada syndrome, a disease with risk of sudden cardiac death. *EBioMedicine* **2020**, *57*, 102843. [CrossRef]
111. Estes, S.I.; Ye, D.; Zhou, W.; Dotzler, S.M.; Tester, D.J.; Bos, J.M.; Kim, C.J.; Ackerman, M.J. Characterization of the CACNA1C-R518C Missense Mutation in the Pathobiology of Long-QT Syndrome Using Human Induced Pluripotent Stem Cell Cardiomyocytes Shows Action Potential Prolongation and L-Type Calcium Channel Perturbation. *Circ. Genom. Precis. Med.* **2019**, *12*, e002534. [CrossRef]
112. Rocchetti, M.; Sala, L.; Dreizehnter, L.; Crotti, L.; Sinnecker, D.; Mura, M.; Pane, L.S.; Altomare, C.; Torre, E.; Mostacciuolo, G.; et al. Elucidating arrhythmogenic mechanisms of long-QT syndrome CALM1-F142L mutation in patient-specific induced pluripotent stem cell-derived cardiomyocytes. *Cardiovasc. Res.* **2017**, *113*, 531–541. [CrossRef] [PubMed]
113. Spencer, C.I.; Baba, S.; Nakamura, K.; Hua, E.A.; Sears, M.A.; Fu, C.-C.; Zhang, J.; Balijepalli, S.; Tomoda, K.; Hayashi, Y.; et al. Calcium Transients Closely Reflect Prolonged Action Potentials in iPSC Models of Inherited Cardiac Arrhythmia. *Stem Cell Rep.* **2014**, *3*, 269–281. [CrossRef] [PubMed]
114. Yazawa, M.; Hsueh, B.; Jia, X.; Pasca, A.M.; Bernstein, J.A.; Hallmayer, J.; Dolmetsch, R.E. Using induced pluripotent stem cells to investigate cardiac phenotypes in Timothy syndrome. *Nat. Cell Biol.* **2011**, *471*, 230–234. [CrossRef] [PubMed]
115. Kiviaho, A.L.; Ahola, A.; Larsson, K.; Penttinen, K.; Swan, H.; Pekkanen-Mattila, M.; Venäläinen, H.; Paavola, K.; Hyttinen, J.; Aalto-Setälä, K. Distinct electrophysiological and mechanical beating phenotypes of long QT syndrome type 1-specific cardiomyocytes carrying different mutations. *IJC Hear. Vasc.* **2015**, *8*, 19–31. [CrossRef]
116. Bezzerides, V.J.; Zhang, A.; Xiao, L.; Simonson, B.; Khedkar, S.A.; Baba, S.; Ottaviano, F.; Lynch, S.; Hessler, K.; Rigby, A.C.; et al. Inhibition of serum and glucocorticoid regulated kinase-1 as novel therapy for cardiac arrhythmia disorders. *Sci. Rep.* **2017**, *7*, 1–13. [CrossRef]
117. Barajas-Martinez, H.; Smith, M.; Hu, D.; Goodrow, R.J.; Puleo, C.; Hasdemir, C.; Antzelevitch, C.; Pfeiffer, R.; Treat, J.A.; Cordeiro, J.M. Susceptibility to Ventricular Arrhythmias Resulting from Mutations in FKBP1B, PXDNL, and SCN9A Evaluated in hiPSC Cardiomyocytes. *Stem Cells Int.* **2020**, *2020*, 1–16. [CrossRef]
118. Liang, P.; Sallam, K.; Wu, H.; Li, Y.; Itzhaki, I.; Garg, P.; Zhang, Y.; Vermglinchan, V.; Lan, F.; Gu, M.; et al. Patient-Specific and Genome-Edited Induced Pluripotent Stem Cell–Derived Cardiomyocytes Elucidate Single-Cell Phenotype of Brugada Syndrome. *J. Am. Coll. Cardiol.* **2016**, *68*, 2086–2096. [CrossRef]
119. El-Battrawy, I.; Müller, J.; Zhao, Z.; Cyganek, L.; Zhong, R.; Zhang, F.; Kleinsorge, M.; Lan, H.; Li, X.; Xu, Q.; et al. Studying Brugada Syndrome With an SCN1B Variants in Human-Induced Pluripotent Stem Cell-Derived Cardiomyocytes. *Front. Cell Dev. Biol.* **2019**, *7*, 261. [CrossRef]
120. Zhang, X.-H.; Morad, M. Calcium signaling in human stem cell-derived cardiomyocytes: Evidence from normal subjects and CPVT afflicted patients. *Cell Calcium* **2016**, *59*, 98–107. [CrossRef]
121. Zhang, X.-H.; Wei, H.; Xia, Y.; Morad, M. Calcium signaling consequences of RyR2 mutations associated with CPVT1 introduced via CRISPR/Cas9 gene editing in human-induced pluripotent stem cell–derived cardiomyocytes: Comparison of RyR2-R420Q, F2483I, and Q4201R. *Hear. Rhythm.* **2020**. [CrossRef]

122. Pölönen, R.P.; Penttinen, K.; Swan, H.; Aalto-Setälä, K. Antiarrhythmic Effects of Carvedilol and Flecainide in Cardiomyocytes Derived from Catecholaminergic Polymorphic Ventricular Tachycardia Patients. *Stem Cells Int.* **2018**, *2018*, 1–11. [CrossRef] [PubMed]
123. Ahola, A.; Pölönen, R.P.; Aalto-Setälä, K.; Hyttinen, J. Simultaneous Measurement of Contraction and Calcium Transients in Stem Cell Derived Cardiomyocytes. *Ann. Biomed. Eng.* **2017**, *46*, 148–158. [CrossRef] [PubMed]
124. Itzhaki, I.; Maizels, L.; Huber, I.; Gepstein, A.; Arbel, G.; Caspi, O.; Miller, L.; Belhassen, B.; Nof, E.; Glikson, M.; et al. Modeling of Catecholaminergic Polymorphic Ventricular Tachycardia With Patient-Specific Human-Induced Pluripotent Stem Cells. *J. Am. Coll. Cardiol.* **2012**, *60*, 990–1000. [CrossRef] [PubMed]
125. Penttinen, K.; Swan, H.; Vanninen, S.; Paavola, J.; Lahtinen, A.M.; Kontula, K.; Aalto-Setälä, K. Antiarrhythmic Effects of Dantrolene in Patients with Catecholaminergic Polymorphic Ventricular Tachycardia and Replication of the Responses Using iPSC Models. *PLoS ONE* **2015**, *10*, e0125366. [CrossRef]
126. Bezzerides, V.J.; Caballero, A.; Wang, S.; Ai, Y.; Hylind, R.J.; Lu, F.; Heims-Waldron, D.A.; Chambers, K.D.; Zhang, D.; Abrams, D.J.; et al. Gene Therapy for Catecholaminergic Polymorphic Ventricular Tachycardia by Inhibition of Ca 2+ /Calmodulin-Dependent Kinase II. *Circulation* **2019**, *140*, 405–419. [CrossRef] [PubMed]
127. Lan, H.; Xu, Q.; El-Battrawy, I.; Zhong, R.; Li, X.; Lang, S.; Cyganek, L.; Borggrefe, M.; Zhou, X.; Akin, I. Ionic Mechanisms of Disopyramide Prolonging Action Potential Duration in Human-Induced Pluripotent Stem Cell-Derived Cardiomyocytes From a Patient With Short QT Syndrome Type 1. *Front. Pharmacol.* **2020**, *11*, 554422. [CrossRef]
128. El-Battrawy, I.; Lan, H.; Cyganek, L.; Zhao, Z.; Li, X.; Buljubasic, F.; Lang, S.; Yücel, G.; Sattler, K.; Zimmermann, W.-H.; et al. Modeling Short QT Syndrome Using Human-Induced Pluripotent Stem Cell–Derived Cardiomyocytes. *J. Am. Hear. Assoc.* **2018**, *7*, 7. [CrossRef]
129. Shinnawi, R.; Shaheen, N.; Huber, I.; Shiti, A.; Arbel, G.; Gepstein, A.; Ballan, N.; Setter, N.; Tijsen, A.J.; Borggrefe, M.; et al. Modeling Reentry in the Short QT Syndrome With Human-Induced Pluripotent Stem Cell–Derived Cardiac Cell Sheets. *J. Am. Coll. Cardiol.* **2019**, *73*, 2310–2324. [CrossRef]
130. Wu, P.; Deng, G.; Sai, X.; Guo, H.; Huang, H.; Zhu, P. Maturation strategies and limitations of induced pluripotent stem cell-derived cardiomyocytes. *Biosci. Rep.* **2020**. [CrossRef]
131. Magdy, T.; Schuldt, A.J.; Wu, J.C.; Bernstein, D.; Burridge, P.W. Human Induced Pluripotent Stem Cell (hiPSC)-Derived Cells to Assess Drug Cardiotoxicity: Opportunities and Problems. *Annu. Rev. Pharmacol. Toxicol.* **2018**, *58*, 83–103. [CrossRef]
132. Marchianò, S.; Bertero, A.; Murry, C.E. Learn from Your Elders: Developmental Biology Lessons to Guide Maturation of Stem Cell-Derived Cardiomyocytes. *Pediatr. Cardiol.* **2019**, *40*, 1367–1387. [CrossRef] [PubMed]
133. Ahmed, R.E.; Anzai, T.; Chanthra, N.; Uosaki, H. A Brief Review of Current Maturation Methods for Human Induced Pluripotent Stem Cells-Derived Cardiomyocytes. *Front. Cell Dev. Biol.* **2020**, *8*, 178. [CrossRef] [PubMed]
134. Gintant, G.; Traebert, M. The roles of human induced pluripotent stem cell-derived cardiomyocytes in drug discovery: Managing in vitro safety study expectations. *Expert Opin. Drug Discov.* **2020**, *15*, 719–729. [CrossRef] [PubMed]
135. Richards, D.J.; Li, Y.; Kerr, C.M.; Yao, J.; Beeson, G.C.; Coyle, R.C.; Chen, X.; Jia, J.; Damon, B.; Wilson, R.; et al. Human cardiac organoids for the modelling of myocardial infarction and drug cardiotoxicity. *Nat. Biomed. Eng.* **2020**, *4*, 446–462. [CrossRef]
136. Jou, C.J.; Barnett, S.M.; Bian, J.-T.; Weng, H.C.; Sheng, X.; Tristani-Firouzi, M. An In Vivo Cardiac Assay to Determine the Functional Consequences of Putative Long QT Syndrome Mutations. *Circ. Res.* **2013**, *112*, 826–830. [CrossRef]
137. Nesmith, H.W.; Zhang, H.; Rogers, J.M. Optical mapping of electromechanics in intact organs. *Exp. Biol. Med.* **2019**, *245*, 368–373. [CrossRef]
138. Várkuti, B.H.; Képiró, M.; Horváth, I.Á.; Végner, L.; Ráti, S.; Zsigmond, Á.; Hegyi, G.; Lenkei, Z.; Varga, M.; Málnási-Csizmadia, A. A highly soluble, non-phototoxic, non-fluorescent blebbistatin derivative. *Sci. Rep.* **2016**, *6*, 26141. [CrossRef]
139. Weber, M.; Scherf, N.; Meyer, A.M.; Panáková, D.; Kohl, P.; Huisken, J. Cell-accurate optical mapping across the entire developing heart. *eLife* **2017**, *6*, e28307. [CrossRef]

140. Kappadan, V.; Telele, S.; Uzelac, I.; Fenton, F.; Parlitz, U.; Luther, S.; Christoph, J. High-Resolution Optical Measurement of Cardiac Restitution, Contraction, and Fibrillation Dynamics in Beating vs. Blebbistatin-Uncoupled Isolated Rabbit Hearts. *Front. Physiol.* **2020**, *11*, 464. [CrossRef]
141. Antinucci, P.; Hindges, R. A crystal-clear zebrafish for in vivo imaging. *Sci. Rep.* **2016**, *6*, 29490. [CrossRef]
142. Lazzari-Dean, J.; Gest, A.M.M.; Miller, E.W. Optical estimation of absolute membrane potential using fluorescence lifetime imaging. *eLife* **2019**, *8*. [CrossRef] [PubMed]

Publisher's Note: MDPI stays neutral with regard to jurisdictional claims in published maps and institutional affiliations.

© 2020 by the authors. Licensee MDPI, Basel, Switzerland. This article is an open access article distributed under the terms and conditions of the Creative Commons Attribution (CC BY) license (http://creativecommons.org/licenses/by/4.0/).